
Article:
Masters, Sarah L., Robertson, Heather E., Wann, Derek A. orcid.org/0000-0002-5495-274X et al. (5 more authors) (2015) Molecular structure of 1,2-bis(trifluoromethyl)-1,1,2,2-tetramethyldisilane in the gas, liquid, and solid phases : Unusual conformational changes between phases. Journal of Physical Chemistry A. pp. 1600-1608. ISSN 1089-5639

https://doi.org/10.1021/jp507744u

Molecular Structure of 1,2-bis(trifluoromethyl)-1,1,2,2-tetramethyldisilane in the Gas, Liquid and Solid Phases – Unusual Conformational Changes Between Phases

Sarah L. Masters,*[,†] Heather E. Robertson,[‡] Derek A. Wann,[§] Margit Hölbling,[∥] Karl Hassler,[∥] Ragnar Bjornsson,[⊥] Sunna Ó. Wallevik,[⊥] and Ingvar Arnason[⊥]

[†] Department of Chemistry, University of Canterbury, Private Bag 4100, Christchurch, 8104, New Zealand.

[‡] School of Chemistry, University of Edinburgh, West Mains Road, Edinburgh, U.K. EH9 3JJ.

[§] Department of Chemistry, University of York, Heslington, York, U.K. YO10 5DD.

∥ Technische Universität Graz, Stremayergasse 16, A-8010 Graz, Austria.

[⊥] Science Institute, University of Iceland, Dunhaga 3, IS-107, Reykjavik, Iceland.

■ AUTHOR INFORMATION

Corresponding Author

* E-mail: sarah.masters@canterbury.ac.nz (S.L.M.)

ABSTRACT: The molecular structure of 1,2-bis(trifluoromethyl)-1,1,2,2-tetramethyldisilane has been determined in three different phases (solid, liquid and gas) using various spectroscopic and diffraction techniques. Both the solid-state and gas-phase investigations revealed only one conformer to be present in the sample analyzed, while the liquid phase revealed the presence of three conformers. The data have been reproduced using computational methods and a rationale is presented for the observation of three conformers in the liquid state.

KEYWORDS: electron diffraction – Raman spectroscopy – X-ray diffraction – disilanes – conformational studies

■ INTRODUCTION

The study of the molecular structures of bulky substituted disilanes has been of interest to the Masters Research group for a number of years. Such systems often adopt unusual conformations in the gas phase because of steric hindrance, revealing interesting information regarding their chemistries and reactivities. Examples include 1,2-di-*tert*-butyldisilane,[1] 1,2-di-*tert*-butyltetrachlorodisilane,[2] 1,1,2-tri-*tert*-butyl-disilane,[3] and 1,1,2,2-tetra-*tert*-butyldisilane[4] which have all previously been studied by gas electron diffraction (GED) supported by *ab initio* calculations using the SARACEN method.[5–7] The structure of 1,2-di-*tert*-butyldisilane[1] was found to be *anti* with C_2 symmetry at room temperature, while 1,2-di-*tert*-butyltetrachlorodisilane[2] returned a *transoid* conformation by both GED and *ab initio* methods. Both of these systems displayed evidence of steric crowding, with larger than average bond angles observed about the silicon atoms. For 1,1,2-tri-*tert*-butyldisilane,[3] three conformers (*syn*, *gauche*, and *antiperiplanar*) were located on the potential energy surface, with the *syn* conformer by far the most stable under the conditions of the experiment. Although intuitively this seems unlikely, examination of the structure revealed that each hydrogen atom attached to silicon was eclipsing a *tert*-butyl group at the opposite end of the molecule. This serves to reduce the steric crowding between the *tert*-butyl groups and, although there is still some steric crowding present, it is much reduced in the *syn* conformation. 1,1,2,2-Tetra-*tert*-butyldisilane[4] displayed a similar phenomenon with an *anticlinal* conformation being observed. The Si–Si–C bond angles to the two *tert*-butyl groups that almost eclipse one another increase to 117.0(5)°, and the Si–Si–C bond angles to the *tert*-butyl groups that eclipse hydrogen atoms reduce to 110.7(7)° (see Figure 1).

Figure 1. Newman projections of the lowest energy conformations of (left) 1,2-di-*tert*-butyldisilane, (middle) 1,1,2-tri-*tert*-butyldisilane, and (right) 1,1,2,2-tetra-*tert*-butyldisilane.

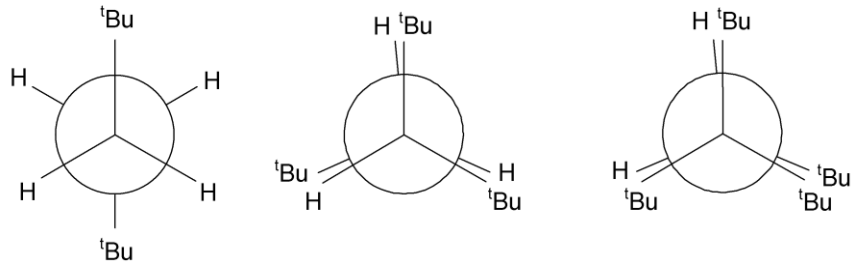

We recently reported the GED-determined structures of 1,1,2,2-tetrakis(trimethylsilyl)disilane and 1,1,2,2-tetrakis(trimethylsilyl)dimethyldisilane, both of which displayed conformational

flexibility in the gas phase.[8] Recent work has also focused on the electronic effect of the substituents. Studies of 1,1,1,2-tetrabromo-2,2-dimethyldisilane[9] and the series of substituted disilane systems [$X_3SiSiMe_3$ (X = H, F, Cl, Br)],[10] also in the gas phase, revealed structural trends that can be attributed to the electronic effects of the substituents. Only one conformer for each of these species was located on the potential-energy surface using *ab initio* methods and this agreed with the conclusions from the GED experiments.

Here, the molecular structure of 1,2-bis(trifluoromethyl)-1,1,2,2-tetramethyldisilane has been studied in the gas phase by GED and *ab initio* methods, in the liquid phase by Raman spectroscopy and *ab initio* methods, and in the solid phase by X-ray diffraction. The results of these investigations are reported and discussed. In particular, this work highlights the differences that the phase can impart on the conformational nature of systems and the importance of awareness and understanding of the phase used to study the molecular structure.

■ EXPERIMENTAL SECTION

Synthesis. CF_3Br (25.1 g, 168.3 mmol) was condensed into a reaction flask containing $(CH_3)_4Si_2Cl_2$ (15.0 g, 80.1 mmol) and CH_2Cl_2 (40 ml). A –78 °C acetone/dry ice bath was placed around the reaction system and, when the content of the flask had reached the bath temperature, a solution of $P(NEt_2)_3$ (39.6 g, 160.3 mmol) in CH_2Cl_2 (30 ml) was added slowly while stirring. The cooling bath was removed and, after continued stirring at room temperature overnight, the colorless solution turned orange. All volatile components were condensed into a trap held at –196 °C. The solvent was distilled off and the product was collected by distillation under nitrogen at 129–130 °C. Yield: 8.83 g, 44% (colorless semi-solid at room temperature); ^{1}H NMR (400.1 MHz, $CDCl_3$, 25 °C, TMS): ∂ = 0.43 (s, 12 H, CH_3), ^{13}C NMR (100.6 MHz, $CDCl_3$, 25 °C, TMS): ∂ = –7.4 (s, CH_3), 132.1 (q, CF_3, J_{CF} = 322 Hz), ^{19}F NMR (376.5 MHz, $CDCl_3$, 25 °C, $CFCl_3$): ∂ = –61.6 (s, $^2J_{FSi}$ = 38.5 Hz), ^{29}Si NMR (79.5 MHz, $CDCl_3$, 25 °C, TMS): ∂ = –13.0 (qq, $^2J_{FSi}$ = 38.5 Hz). The sample was then used without further purification for the GED experiment.

Computational Methods. All calculations at the HF and MP2 levels were performed using the resources of the EaStCHEM research computing facility,[11] and the National Service for Computational Chemistry Software,[12] utilising the Gaussian03 program.[13] Potential-energy surface scans were performed at the HF level with the 6-31G* basis set,[14] and at the MP2 level with the 6-31G*, 6-311G*,[15] 6-311+G* and aug-cc-pVDZ[16] basis sets to determine the number of conformers present at each of the different levels. Geometry optimizations were

then performed for each of the minima on the respective potential-energy surfaces at all combinations of level of theory and basis set.

Analytic second derivatives of the energy with respect to nuclear coordinates calculated at the MP2/6-31G* level gave the force field for the lowest energy conformer. These were used in the program SHRINK[17,18] to provide estimates of the amplitudes of vibration (u) and perpendicular distance corrections (k) for use in the GED refinement. As harmonic force constants were calculated, the refinement type is denoted r_{h1}.[19]

In addition, the SMD solvation model[20] as implemented in ORCA (version 3.0.2)[21] was used in conjunction with DFT calculations at the B3LYP-D3BJ/def2-TZVP level[22–28] to explore the potential-energy surface of 1,2-bis(trifluoromethyl)-1,1,2,2-tetramethyldisilane in solution with the aim of understanding the liquid-phase Raman spectroscopic data.

Gas Electron Diffraction (GED). Data were collected for 1,2-bis(trifluoromethyl)-1,1,2,2-tetramethyldisilane using the GED apparatus formerly housed at the University of Edinburgh.[29] An accelerating voltage of *ca.* 40 kV (electron wavelength *ca.* 6.0 pm) was used, whilst maintaining the sample and nozzle temperatures at 293 K. Scattering intensities were recorded at nozzle-to-plate distances of 127.5 and 285.3 mm on Kodak Electron Image plates. The electron-scattering intensities were measured using an Epson Expression 1680 Pro flatbed scanner and converted to mean optical densities as a function of the scattering variable, s, using an established program.[30] The data reduction and least-squares refinement processes were carried out using the ed@ed program[31] (version 2.3) employing the scattering factors of Ross *et al.*[32] The weighting for the off-diagonal weight matrices, correlation parameters, and scale factors for the two camera distances are given in Table S1, together with electron wavelengths, which were determined from the scattering patterns of benzene vapor. These were recorded immediately after the compound patterns and analyzed in exactly the same way, to minimize systematic errors in wavelengths and camera distances.

Temperature-Dependent Raman Spectroscopy. Raman spectra were recorded with a Jobin Yvon T64000 spectrometer equipped with a triple monochromator and a CCD camera. Spectra were recorded in the subtractive mode with a resolution of 3 cm^{-1}. The samples were held in 1 mm glass capillary tubes and irradiated by the green 532 nm line of a frequency-doubled Nd-YAG laser (Coherent, DPSS Model 532-20, 10 mW). Spectra were recorded for the pure compound and for a solution in cyclopentane. A continuous flow cryostat (Oxford instruments OptistatCF^{TM}) using liquid nitrogen for cooling was employed for the low-temperature measurements.

The vant't Hoff relationship in the form shown in Equation 1 was used to extract enthalpy differences from the temperature-dependent Raman spectra.

$$\ln\left(\frac{A_1}{A_2}\right) = \frac{-\Delta H}{RT} + \frac{\Delta S}{R} + c \qquad (1)$$

Here, A_1 and A_2 denote intensities of bands belonging to conformers 1 and 2, respectively; peak areas have been used for this purpose. As the ratio of the Raman scattering coefficients (α_1 and α_2) is included in the constant, c, ΔH and ΔS are independent of temperature, and a linear relation is obtained by plotting the logarithm of the intensity ratio against the inverse temperature.

X-ray diffraction (XRD). The disilane was crystallized from a solution in cyclopentane using an Optical Heating and Crystallization Device (OHCD) from SciConcept. The solution was transferred into a 0.2 mm glass capillary, which was sealed with an epoxide adhesive at both ends. The capillary was fixed with wax in a brass mount, which then was transferred to the goniometer and cooled to 150 K. At this temperature the solution solidified to an amorphous glass. Using an infrared laser, the glassy solid was annealed to remove dissolved gases (nitrogen), before the capillary was then allowed to warm up to 188 K and was again annealed with reduced laser power. After two hours, the sample was screened by X-ray diffraction, revealing the formation of crystals of $(CF_3SiMe_2)_2$ from the cyclopentane solution. Diffuse reflections showed that upon cooling to 173 K, performed with the intention to solidify the solvent and fix the crystals, part of the solvent had crystallized. The X-ray diffraction experiment was subsequently performed at 190 K with a crystal of $(CF_3SiMe_2)_2$ adhered to the capillary wall.

The unit cell contains two formula units of the disilane in the space group $P2_1/n$. The two CF_3 groups are in *antiperiplanar* positions with no evidence of disorder in the crystal. In the difference Fourier map three protons could be localized for each methyl group; they were attached to the carbon atoms using a riding model. The data reveal small F···H interactions between the molecules, with distances between 280 and 286 pm.

Data were collected on a Bruker KAPPA8 APEXII instrument with use of Mo Kα (λ = 0.71073 Å) radiation and a CCD area detector. The SHELX (version 6.1) program package was used for the structure solution and refinement.[33] Absorption corrections were applied using the SADABS program.[34] The crystal structures were solved by direct methods and

refined by full-matrix least-squares procedures. All non-hydrogen atoms were refined anisotropically, while hydrogen atoms were included in the refinement at calculated positions using a riding model as implemented in the SHELXTL program. Crystallographic data have been deposited with the Cambridge Crystallographic Data Centre as supplementary publication no. CCDC-1015708. Copies of the data can be obtained free of charge on application to The Director, CCDC, 12 Union Road, Cambridge CB2 1ET, U.K. (E-mail: deposit@ccdc.cam.ac.uk).

■ RESULTS AND DISCUSSION

Temperature-Dependent Raman Spectroscopy. About fourteen years ago, one of the authors (K.H.) briefly reported the existence of three conformers of $(CF_3SiMe_2)_2$: *gauche*, *ortho*, and *anti*, with backbone dihedral angles of about ±56°, ±101° and ±171°, respectively.[35] The result was derived from a combined *ab initio* and Raman spectroscopic study, which included MP2/6-31G* calculations of conformer stabilities as well as temperature-dependent Raman spectra of the pure compound in the temperature range 318–373 K.

In the present study we report the Raman spectra recorded from a cyclopentane solution. Figure 2 shows the room-temperature spectrum of the solution (red) as well as the spectrum recorded at 225 K (purple) in the wavenumber range 200–800 cm^{-1}, which is free from solvent peaks. Clearly, two bands located at around 300 and 380 cm^{-1} drastically change their shapes upon cooling. Each of the band systems is composed of three overlapping lines and these collapse into a single band at 225 K. At that temperature crystals of $(CF_3SiMe_2)_2$ have formed which, according to the results of X-ray diffraction analysis, are composed solely of the *anti* conformer with a dihedral angle of exactly 180°.

Figure 2. Raman spectrum of a cyclopentane solution of $(CF_3SiMe_2)_2$ at room temperature (red) and at 225 K (purple).

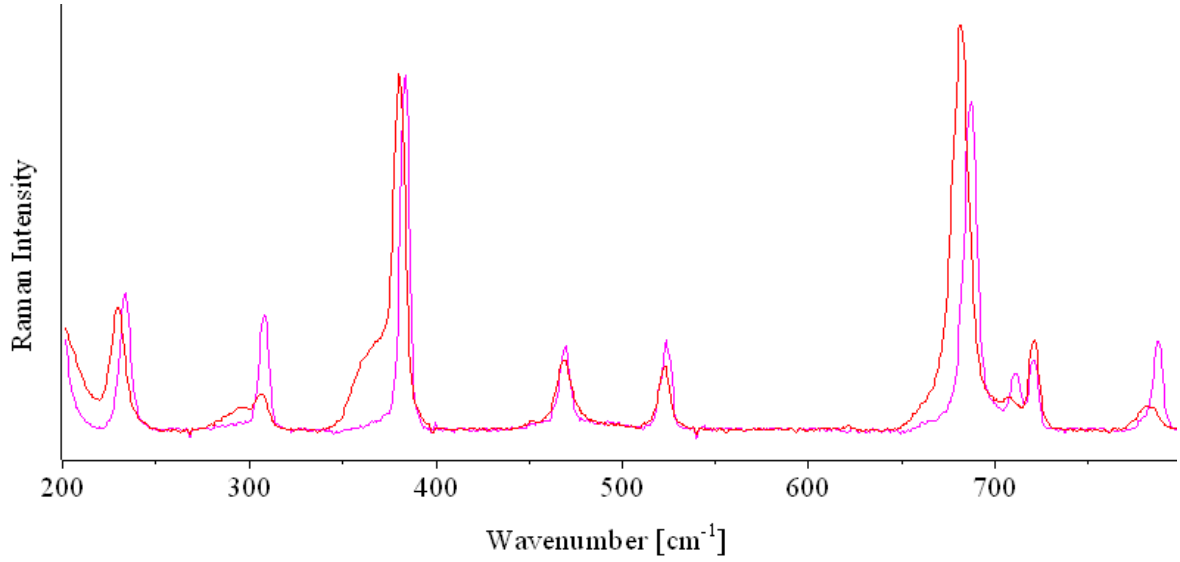

Figure 3 shows the appearance of the 380 cm^{-1} line at 300, 240, and 225 K. Upon cooling from room temperature, the shoulders at 370 and 360 cm^{-1} clearly lose intensity and disappear completely upon crystallization at 225 K. As these intensity changes are reversible with rising temperature they can only originate from rotational isomerism, despite the fact that MP2 calculations with larger basis sets predict the existence of just a single conformer.

The MP2/6-31G* calculations predict that the $SiC(F_3)$ stretching mode at around 360–380 cm^{-1} is sensitive to molecular conformations and possesses a Raman intensity sufficient for detection of the isomers. The predicted wavenumbers are 369 cm^{-1} (*gauche*), 380 cm^{-1} (*ortho*), and 393 cm^{-1} (*anti*), which correlate well with the observed wavenumbers 360, 369, and 380 cm^{-1} obtained from a deconvolution of the band system.

Figure 3. Appearance of the $SiC(F_3)$ stretching vibration for different temperatures. The band at 380 cm^{-1} has been normalized to facilitate comparison of relative intensities. A small wavenumber shift with temperature is also observed.

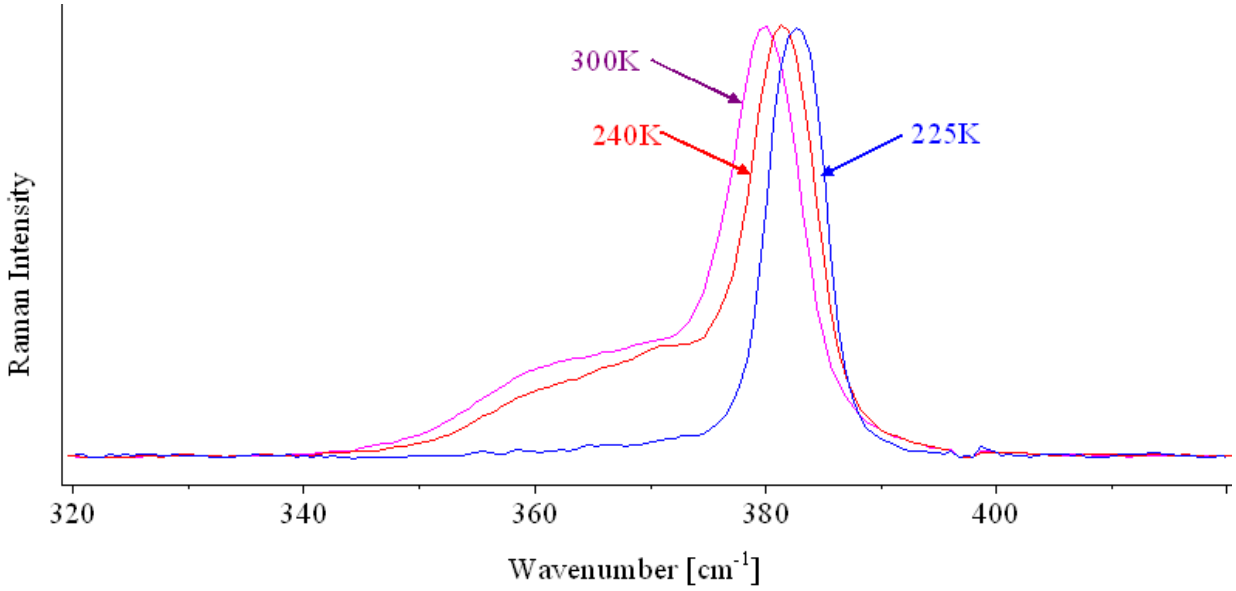

Deconvolution was also employed for the determination of band intensities, which were then used to generate the van't Hoff plots. For illustrative purposes, Figure 4 presents the van't Hoff plot for the band pair 360/380 cm^{-1} for the temperature range 300–240 K. Results for the range 300–380 K are very similar.

Figure 4. Van't Hoff plot for the band pair 360/380 cm^{-1}.

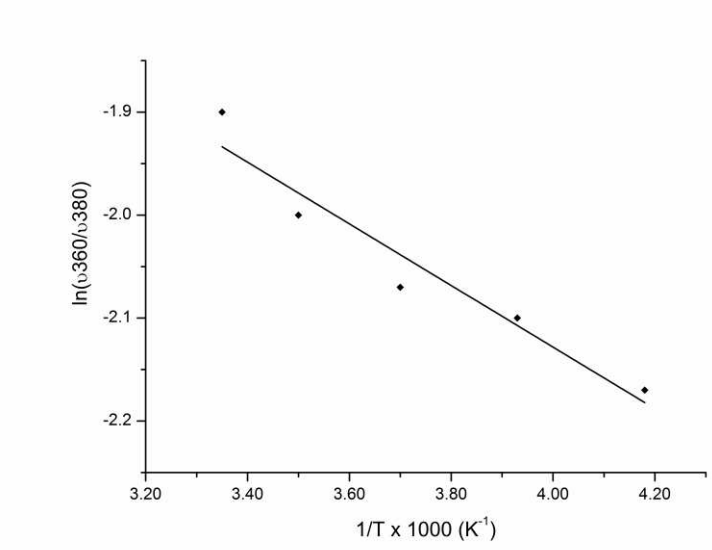

From the van't Hoff plots, relative enthalpies of 0.0, 0.5, and 5.4 kJ mol^{-1} were derived for the *anti*, *ortho*, and *gauche* conformers, respectively. Due to the inherent difficulties of the deconvolution process, the accuracy of these values is not better than ±30–50%.

Computational Studies. From the potential-energy scans about the $F_3C–Si–Si–CF_3$ dihedral angle (Figure 5), it can be seen that there is a definite energy minimum (at 180°) when calculated at the HF/6-31G* level, with possible further minima at the *synclinal* and *anticlinal* positions. At the MP2 level of theory, though still using the 6-31G* basis set, the potential-energy scan yielded three conformers: *synclinal* [ϕC(16)–Si(2)–Si(1)–C(7) = 55.7°], *anticlinal* [ϕC(16)–Si(2)–Si(1)–C(7) = 101.1°], and *antiperiplanar* [ϕC(16)–Si(2)–Si(1)–C(7) = 170.9°] (Figure 6 shows Newman projections of these three). However, on changing the basis set used the number of minima observed also changed. At the MP2 level with 6-311G* the *synclinal* minimum was less pronounced, although the *anticlinal* [ϕC(16)–Si(2)–Si(1)–C(7) = 105.9°] and *antiperiplanar* [ϕC(16)–Si(2)–Si(1)–C(7) = 164.5°] conformers were still present. The same happened with the *anticlinal* minimum at the MP2/6-311+G* level, leaving only the *antiperiplanar* [ϕC(16)–Si(2)–Si(1)–C(7) = 171.6°] minimum. The aug-cc-pVDZ basis set was then used to verify whether the *antiperiplanar* conformer was indeed the only real structure and again only a definite *antiperiplanar* minimum [ϕC(16)–Si(2)–Si(1)–C(7) = 170.0°] was found. The potential-energy plot shows less steep slopes where the other two minima once were.

Figure 5. Potential-energy scans of ϕC(16)–Si(2)–Si(1)–C(7) at HF/6-31G* (yellow), MP2/6-31G* (green), MP2/6-311G* (red), MP2/6-311+G* (blue), and MP2/aug-cc-pVDZ (purple). For clarity, the scans are offset in 0.5 kJ mol^{-1} increments.

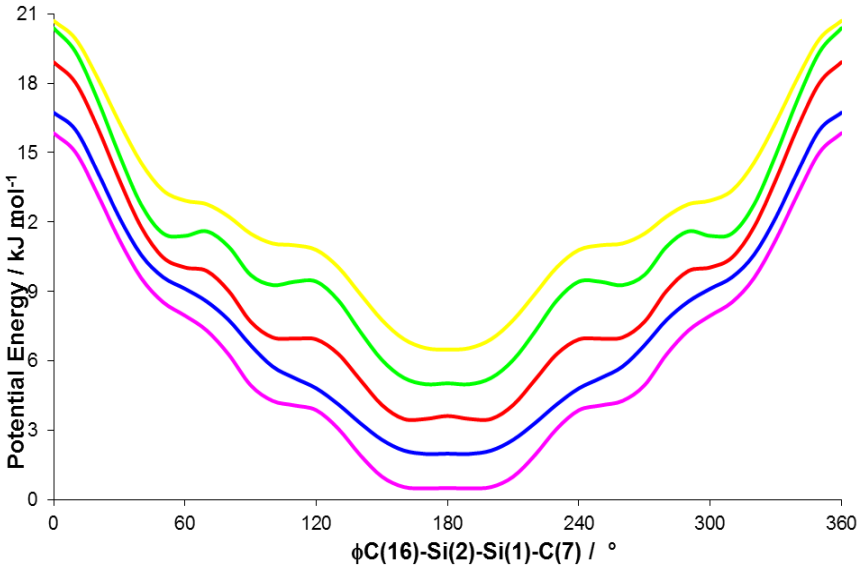

Figure 6. Newman projections of the different conformers: (left) *synclinal* (middle) *anticlinal* and (right) *antiperiplanar*.

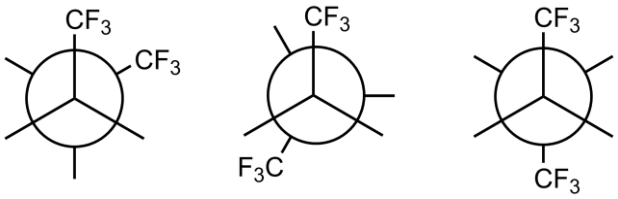

Based on the belief that there was only one minimum on the potential-energy surface in the gas phase, geometry optimizations were performed at the MP2 level using all basis sets and the molecule was found to have C_2 symmetry. As the calculated values for the F_3C–Si–Si–CF_3 dihedral angle for the *antiperiplanar* conformer varied greatly, diffuse basis sets were also used to try and find a converged value. It can be seen in Table 1 that this does not happen. The molecular structure of the lowest energy conformer of 1,2-bis(trifluoromethyl)-1,1,2,2-tetramethyldisilane with atom numbering is given in Figure 7.

Table 1. Bond Angles and Dihedral Angles for the *Antiperiplanar* Conformer of 1,2-bis(trifluoromethyl)-1,1,2,2-tetramethyldisilane Using the MP2 Method with Different Basis Sets[a]

	MP2					
	6-31G*	6-311G*	6-311+G*	6-311++G**	aug-cc-pVDZ	aug-cc-pVTZ
∠C(8)–Si(2)–Si(1)	112.7	112.5	112.6	112.1	111.9	112.9
∠C(3)–Si(2)–Si(1)	113.0	113.3	113.5	113.9	113.2	112.9
∠C(7)–Si(2)–Si(1)	103.8	104.4	104.0	104.2	103.6	104.1
∠F(22)–C(16)–Si(1)	112.1	112.3	112.3	112.4	112.3	112.2
∠F(23)–C(16)–Si(1)	113.9	113.1	113.3	113.3	113.7	113.2
∠F(21)–C(16)–Si(1)	111.3	111.8	112.0	111.8	111.9	112.2
∢C(16)–Si(1)–Si(2)–C(7)	170.9	164.5	171.6	162.0	170.0	180.0

[a] All bond angles and dihedral angles are in degrees.

Figure 7. Molecular structure of the lowest energy conformer of 1,2-bis(trifluoromethyl)-1,1,2,2-tetramethyldisilane with atom numbering.

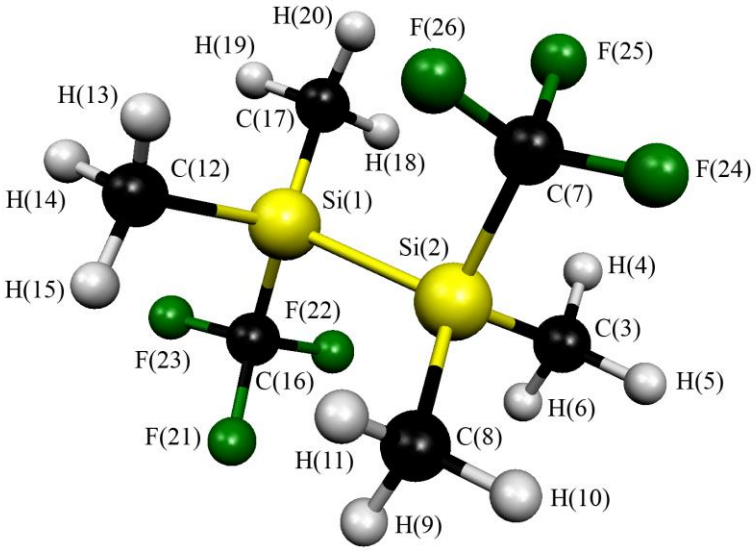

For many of the angles reported in Table 1 their values change little with varying basis set. It is interesting to note that ∠Si–Si–C between the carbon atoms from the trifluoromethyl groups and the two silicon atoms [∠C(16)–Si(1)–Si(2)] were significantly narrower (8–9°) than the corresponding angle for the methyl groups [C(12/17)–Si(1)–Si(2)]. This is due to the highly electronegative fluorine atoms being attracted to the more electropositive silicon centers. The methyl groups are forced to bend away from the silicon center due to steric hindrance from the opposing trifluoromethyl group and to compensate for the narrowing of the Si–Si–C(F_3) angle. At the MP2/6-311++G** level there was also a difference between the two Si–Si–C(H_3) angles. This 2° variation could be due to the two methyl groups being staggered in order to reduce the interaction between them. However, results from the MP2/aug-cc-pVTZ calculation showed that the angles average to 112.9°. This is wider than the corresponding Si–Si–C angles obtained for hexamethyldisilane (108.4±0.4°),[36] demonstrating that the trifluoromethyl groups affect the overall structure of the molecule and not just angles to fluorine atoms.

Table 2. Bond Lengths for the *Antiperiplanar* Conformer Using the MP2 Method with a Variety of Basis Sets[a]

	MP2					
	6-31G*	6-311G*	6-311+G*	6-311++G**	aug-cc-pVDZ	aug-cc-pVTZ
Si–Si	234.1	234.7	235.1	235.3	235.9	235.4
C–H	109.4	109.3	109.4	109.5	110.2	109.0
Si(1)–C(12)	188.0	187.3	187.2	187.3	188.7	187.3
Si(1)–C(17)	188.0	187.2	187.2	187.2	188.7	187.3
Si(1)–C(16)	193.0	193.2	193.9	193.9	194.8	194.1
C(16)–F(21)	137.1	136.1	136.2	136.3	137.8	135.8
C(16)–F(22)	136.7	135.7	136.0	135.9	137.5	135.8
C(16)–F(23)	136.1	135.4	135.6	135.6	137.1	135.3

[a] All bond lengths are in pm.

The calculated Si(1)–Si(2) bond length from each of the levels of calculation (average 235.1 pm) is longer than that obtained from a GED study of Si_2H_6 [233.1(3) pm].[37] The longer central bond is due to the electron-withdrawing capabilities of the fluorine atoms of the two highly electronegative trifluoromethyl groups. This is also the reason for the increased length of the Si(1)–C(16) bond to the trifluoromethyl group (194.1 pm at MP2/aug-cc-pVTZ) compared to the Si(1)–C(12) and Si(1)–C(17) distances to the methyl group (both 187.3 pm at MP2/aug-cc-pVTZ). It is interesting to note that the C–F distances to the extreme fluorine atoms produce different results to those for the fluorine atoms pointing to the center of the molecule. The difference can be attributed to the lack of steric hindrance from the methyl groups on the opposing silicon atom.

A separate continuum-solvation DFT study was undertaken to explore whether solvent effects might be responsible for the conformational behavior seen in the Raman spectra but not in the gas-phase MP2 calculations. The F_3C–Si–Si–CF_3 dihedral angle was scanned from 180 to 0° for an isolated molecule as well as including continuum solvation with the SMD solvation model as implemented in ORCA using the solvent parameters of cyclopentane. Results are shown in Figure 8. The gas-phase B3LYP-D3BJ curve shows a fairly similar energy profile shape to the results of the MP2 calculations in Figure 5, with the *synclinal* (~50°) and *anticlinal* (~100°) regions being rather higher in energy than the *antiperiplanar* region. It is not completely obvious whether the features in the *synclinal* and *anticlinal* regions correspond to true minima due to the flatness of the potential-energy surface at these points.

Figure 8. B3LYP-D3BJ computed energies for 1,2-bis(trifluoromethyl)-1,1,2,2-tetramethyldisilane from relaxed surface scans of the $F_3C–Si–Si–CF_3$ dihedral angle. Scans were performed in gas phase, cyclopentane SMD-solution, and water SMD-solution.

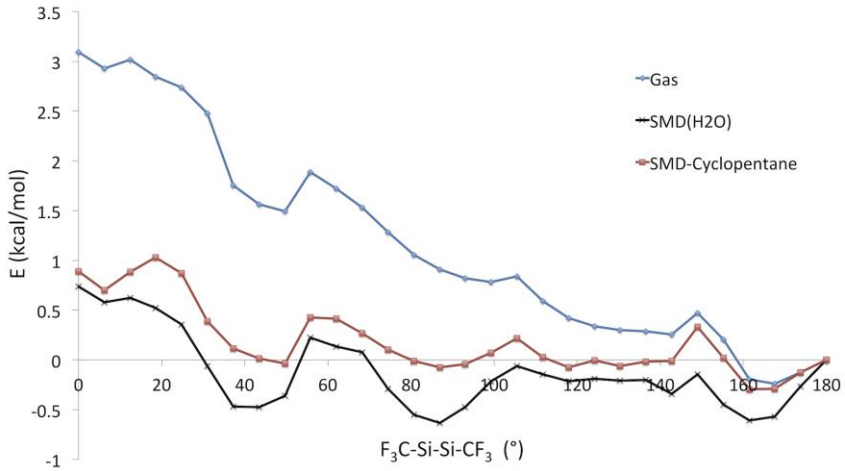

Including continuum solvation in the form of the COSMO-SMD solvation model with the solvent parameters of cyclopentane (dielectric constant of 1.97), however, changes the potential-energy surface considerably as the *synclinal* and *anticlinal* regions are lowered in energy with respect to the *antiperiplanar* conformer. Based on this solvent-corrected conformational energy surface it now seems reasonable to expect population of all three conformers.

The reason for the large solvent effect appears to be related to the dipole moment of the conformers. While the *antiperiplanar* conformer has almost no dipole moment, a dipole moment is created as we step the $F_3C–Si–Si–CF_3$ dihedral away from 180°, reaching a maximum as the dihedral angle approaches 0°, as seen in Figure 9. The larger the dipole moment for a given conformer, the stronger the solute-solvent interaction will be, resulting in stabilization of the higher dipole conformers.

Figure 9. B3LYP-D3BJ computed dipole moment (Debye) of 1,2-bis(trifluoromethyl)-1,1,2,2-tetramethyldisilane as a function of the $F_3C–Si–Si–CF_3$ torsion. Data were obtained by relaxed surface scans in the gas phase, cyclopentane SMD-solution, and water SMD-solution.

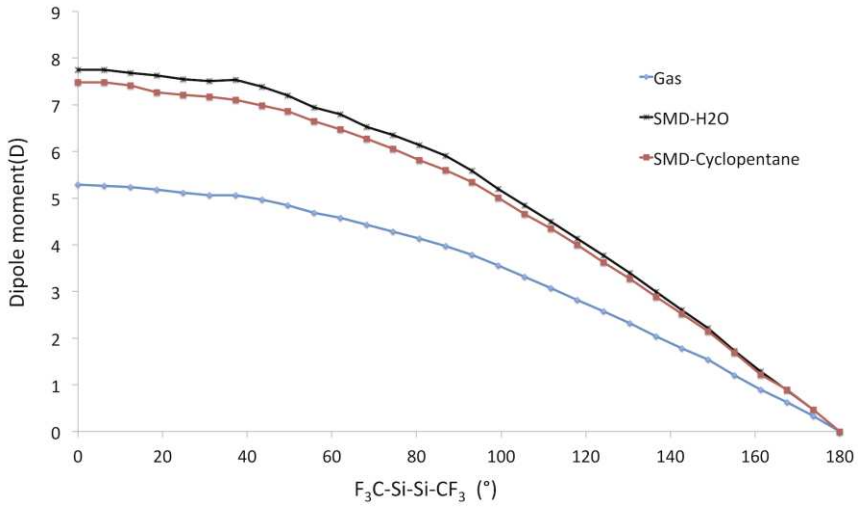

In order to confirm this explanation of the changes of the conformational energy surface we performed COSMO-SMD calculations in water which has an even higher dielectric. We would expect a larger stabilization of the region of the surface with higher dipole moment. This is indeed observed, as shown in Figure 8, where the curve for water reveals an even larger stabilization of the *synclinal* and *anticlinal* regions. Wells in the potential-energy profile are now even better resolved and separate geometry optimizations confirm the three conformers as true minima.

We note that accurate solvation energies are difficult to predict by continuum solvation models, which will always be crude representations of the real solvent environment. However, the trend towards stabilization of the *synclinal* and *anticlinal* conformers as a function of dielectric constant (which is connected to the molecular dipole moment) is the most important observation.

Gas Electron Diffraction (GED). GED refinements were carried out for 1,2-bis(trifluoromethyl)-1,1,2,2-tetramethyldisilane based on the *ab initio* calculations described above (optimized at the MP2/6-311++G** level), using a model with C_2 point-group symmetry. The structure was defined in terms of twelve independent geometric parameters described in the Supporting Information.

Theoretical Cartesian force fields were generated at the MP2/6-31G* level and converted to a set of force fields described by a set of symmetry coordinates, after which root-mean-

square (RMS) amplitudes of vibration were obtained from the SHRINK program.[17,18] All independent geometric parameters were refined using a least-squares method and restraints were applied, using the SARACEN method,[5–7] to five parameters that could otherwise not be refined (Table 4). The restraints were based on values calculated at the MP2/6-311++G** level. In addition, 16 groups of amplitudes of vibration were refined (see Table S2). The success of the refinement can be assessed numerically using the final *R* factor,[9] which was R_G = 0.042 (R_D = 0.027), and visually using the radial-distribution and difference curves (Figure 10), and the molecular-scattering intensity curves (Figure S1). The least-squares correlation matrix is given in Table S3 and coordinates for the final GED structure and for the calculated structure (MP2/6-311++G**) are in Tables S4 and S5, respectively.

Table 4. Refined and Calculated Parameters for GED Refinement of $(H_3C)_2(F_3C)Si–Si(CF_3)(CH_3)_2$[a]

Parameters		GED (r_{h1})	MP2/6-311++G** (r_e)	restraint
Independent				
p_1	*r*Si–C average	190.19(7)	190.6	—
p_2	*r*Si–C difference	6.8(2)	6.7	6.7(5)
p_3	*r*Si–Si	236.4(4)	235.3	—
p_4	*r*C–H	109.6(2)	109.5	109.5(5)
p_5	*r*C–F	135.57(4)	135.8	—
p_6	∠Si–C–H average	111.3(7)	110.8	110.8(10)
p_7	∠Si–C–F average	112.84(6)	112.5	—
p_8	∠C–Si–C	106.1(2)	106.4	106.4(10)
p_9	∠Si–Si–C(F_3)	104.6(3)	104.2	—
p_{10}	∠Si–Si–C(H_3) average	112.3(3)	113.0	—
p_{11}	∠Si–Si–C(H_3) difference	1.7(5)	1.8	1.8(5)
p_{12}	ϕC(16)–Si(1)–Si(2)–C(7)	171.5(31)	160.0	—
Dependent				
p_{13}	*r*Si(1)–C(12)	186.81(8)	187.3	—
p_{14}	*r*Si(1)–C(17)	186.81(8)	187.2	—
p_{15}	*r*Si(1)–C(16)	193.6(2)	193.9	—
p_{16}	∠Si(2)–Si(1)–C(12)	111.5(3)	112.1	—

p_{17}	∠Si(2)–Si(1)–C(17)	113.1(3)	113.9	—
p_{18}	∠Si(2)–Si(1)–C(16)	104.6(3)	104.2	—

[a] Distances (r_{h1}) are in pm and bond angles (∠) and dihedral angles (ϕ) are in degrees.

Figure 10. Experimental, theoretical and difference (experimental – theoretical) radial distribution curves for 1,2-bis(trifluoromethyl)-1,1,2,2-tetramethyldisilane.

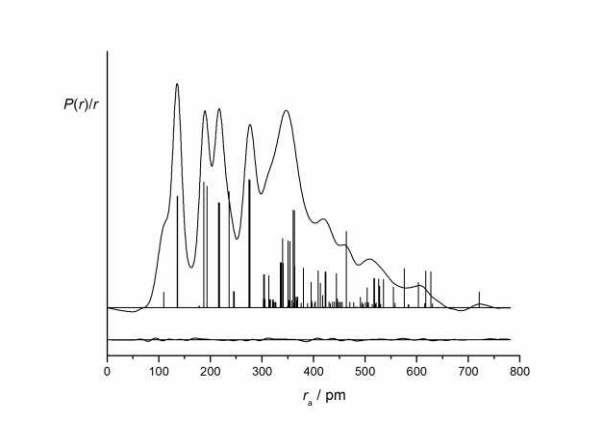

Comparison of Structural Data from Different States. Evidence from theoretical methods shows that 1,2-bis(trifluoromethyl)-1,1,2,2-tetramethyldisilane exists solely as the *antiperiplanar* conformer in the gaseous phase. The experimental data are consistent with one conformer, although more conformers cannot be ruled out entirely. The GED data were fitted using the SARACEN method[5–7] based on this *antiperiplanar* structure.

The final refined structure is in reasonable agreement with MP2/6-311++G** *ab initio* calculations (Table 4). For example, the calculated Si–Si bond length was 235.3 pm compared to 236.4(4) pm from the GED experiment. The observed Si–C(H_3) bond length [186.81(8) pm] compares well to the Si–C lengths in tetramethyldisilane (187.5±0.2 pm) and hexamethyldisilane (187.7±0.2 pm).[36] However, the Si–C(F_3) bond distance shows significant elongation to 193.6(2) pm. This is a significant difference and demonstrates the electronic effects on Si–C bonds due to the addition of fluorine atoms on the ligands.

The observed F_3C–Si–Si–CF_3 dihedral angle [171.5(31)°] was rather different to that calculated at MP2/6-311++G** (160.0°). However, this is in fact very close to the angles calculated at MP2/6-31G*, MP2/6-311+G*, and MP2/aug-cc-pVDZ levels and a variation of just over 10° corresponds to only around three standard deviations.

The gas-phase structure of 1,2-bis(trifluoromethyl)-1,1,2,2-tetramethyldisilane was observed to adopt the same conformation as that in the solid state. As expected, due to the

differences in measurement technique, structural parameters relating to bond lengths were shorter for the crystalline structure. For example, the Si–Si bond length was 234.66(12) pm compared to the gaseous value of 236.4(4) pm. The Si–C bond lengths in the crystal were also observed to be shorter at 185.5(3) and 192.3(2) pm compared to 186.81(8) pm and 193.6(2) pm in the gas phase. The bond angles generally agreed well. The main difference between the structures is observed for ϕC(16)–Si(1)–Si(2)–C(7), which is 180.0° in the solid state but refines to a value of 171.5(31)° in the GED refinement. However, these values are close enough to make the observation that the same conformer is observed in the solid and gaseous phases.

The Raman spectra at 240 and 300 K (Figure 3) reveal broadened peaks at 360–380 cm^{-1} that can be assigned as vibrations due to three different conformers. Three conformers have been located by both MP2 and DFT calculations and their vibrational frequencies and Raman intensities are in good agreement with the experimental data. As these are high-energy conformers on the gas-phase conformational-energy surface and, as both GED data and crystal structure data suggest only a single dominant conformer, there would seem to be an inconsistency. We have demonstrated, however, using a modern continuum solvation model that the higher energy conformers should be stabilized in solution due to their larger dipole moments compared to the *antiperiplanar* conformer, thus populating all three conformers in solution to some extent.

■ ASSOCIATED CONTENT

Supporting Information

Experimental parameters for the GED refinements (Table S1); refined and calculated RMS amplitudes of vibration, distance corrections, and associated r_a distances from the GED refinement for the title molecule (Table S2); least-squares correlation matrix from the GED refinement (Table S3); calculated Cartesian coordinates for the title molecule (Table S4); Cartesian coordinates from the GED refinement for the title molecule (Table S5); molecular scattering intensities and difference curves from the GED refinement (Figures S1). This material is available free of charge via the Internet at http://pubs.acs.org.

■ ACKNOWLEDGMENTS

We thank the EPSRC for funding the gas electron diffraction research (grant EP/C513649) and a Fellowship for D.A.W. (EP/I004122). This work has made use of the resources provided by the EaStCHEM Research Computing Facility.

(http://www.eastchem.ac.uk/rcf) This facility is partially supported by the eDIKT initiative. (http://www.edikt.org.) The authors would like to acknowledge the use of the EPSRC UK National Service for Computational Chemistry Software (NSCCS) at Imperial College London in carrying out this work.

■ REFERENCES

1. Hnyk, D.; Fender, R. S.; Robertson, H. E.; Rankin, D. W. H.; Bühl, M.; Hassler, K.; Schenzel, K. An electron diffraction, ab initio and vibrational spectroscopic study of 1,2-di-*tert*-butyldisilane. *J. Mol. Struct.* **1995**, *346*, 215-229.
2. Hinchley, S. L.; Smart, B. A.; Morrison, C. A.; Robertson, H. E.; Rankin, D. W. H.; Coxall, R. A.; Parsons, S.; Zink, R.; Siegl, H.; Hassler, K.; Mawhorter, R. Molecular structure of $Bu^tCl_2SiSiCl_2Bu^t$ in the gas phase by electron diffraction and *ab initio* calculations. Molecular structures of the compounds $Bu^tX_2SiSiX_2Bu^t$ (X = Cl, Br or I) by vibrational spectroscopy, X-ray crystallography and *ab initio* calculations. *J. Chem. Soc., Dalton Trans.* **2001**, 2916-2925.
3. Hinchley, S. L.; Smart, B. A.; Morrison, C. A.; Robertson, H. E.; Rankin, D. W. H.; Zink, R.; Hassler, K. 1,1,2-Tri-*tert*-butyldisilane, $Bu^t_2HSiSiH_2Bu^t$: vibrational spectra and molecular structure in the gas phase by electron diffraction and *ab initio* calculations. *J. Chem. Soc., Dalton Trans.* **1999**, 2303-2310.
4. Hinchley, S. L.; Robertson, H. E.; Parkin, A.; Rankin, D. H. W.; Tekautz, G.; Hassler, K. Molecular structure of 1,1,2,2-tetra-*tert*-butyldisilane: unusual structural motifs in sterically crowded disilanes. *Dalton Trans.* **2004**, 759-766.
5. Blake, A. J.; Brain, P. T.; McNab, H.; Miller, J.; Morrison, C. A.; Parsons, S.; Rankin, D. W. H.; Robertson, H. E.; Smart, B. A. Structure analysis restrained by *ab initio* calculations: the molecular structure of 2,5-dichloropyrimidine in gaseous and crystalline phases. *J. Phys. Chem.* **1996**, *100*, 12280-12287.
6. Brain, P. T.; Morrison, C. A.; Parsons, S.; Rankin, D. W. H. Tetraborane(10), B_4H_{10}: Structures in Gaseous and Crystalline Phases. *J. Chem. Soc., Dalton Trans.* **1996**, 4589-4596.
7. Mitzel, N. W.; Rankin, D. W. H. SARACEN – Molecular Structures from Theory and Experiment: the Best of Both Worlds. *Dalton Trans.* **2003**, 3650-3662.
8. Schwabedissen, J.; Lane, P. D.; Masters, S. L.; Hassler, K.; Wann, D. A. Gas-phase structures of sterically crowded disilanes studied by electron diffraction and

quantum chemical methods: 1,1,2,2-tetrakis(trimethylsilyl)disilane and 1,1,2,2-tetrakis(trimethylsilyl)dimethyldisilane. *Dalton Trans.* **2014**, *43*, 10175-10182.

9. Masters, S. L.; Atkinson, S. J.; Hölbling, M.; Hassler, K. Gas-phase molecular structure of 1,1,1,2-tetrabromo-2,2-dimethyldisilane: theoretical and experimental investigation of a super-halogenated disilane and computational investigation of the F, Cl and I analogues. *Struct. Chem.* **2013**, *24*, 1201-1206.
10. Atkinson, S. J.; Robertson, H. E.; Hölbling, M.; du Mont, W.-W.; Mitrofan, C.; Hassler, K.; Masters, S. L. Do halogen and methyl substituents have electronic effects on the structures of simple disilanes? An experimental and theoretical study of the molecular structures of the series $X_3SiSiMe_3$ (X = H, F, Cl and Br). *Struct. Chem.* **2013**, *24*, 851-857.
11. http://www.eastchem.ac.uk/rcf
12. http://www.nsccs.ac.uk
13. Frisch, M. J.; Trucks, G. W.; Schlegel, H. B.; Scuseria, G. E.; Robb, M. A.; Cheeseman, J. R.; Montgomery, J. A., Jr.; Vreven, T.; Kudin, K. N.; Burant, J. C. *et al*. *Gaussian 03, Revision C.01*; Gaussian, Inc.; Wallingford, CT, 2004. See Supporting Information for full reference text.
14. Gordon, M. S. The isomers of silacyclopropane. *Chem. Phys. Lett.* **1980**, *76*, 163-168; Hariharan, P. C., Pople, J. A. Influence of polarization functions on MO hydrogenation energies. *Theor. Chim. Acta.* **1973**, *28*, 213-222; Hehre, W. J., Ditchfield, R., Pople, J. A. Self-consistent molecular orbital methods. XII. Further extensions of Gaussian-type basis sets for use in molecular orbital studies of organic molecules. *J. Chem. Phys.* **1972**, *56*, 2257–2261.
15. Krishnan, R., Binkley, J. S., Seeger, R., Pople, J. A. Self-consistent molecular orbital methods. XX. A basis set for correlated wave functions. *J. Chem. Phys.* **1980**, *72*, 650-654; McLean, A. D., Chandler, G. S. Contracted Gaussian-basis sets for molecular calculations. 1. Second row atoms, Z = 11–18. *J. Chem. Phys.* **1980**, *72*, 5639-5648.
16. Kendall, R. A., Dunning Jr., T. H., Harrison, R. J. Electron affinities of the first-row atoms revisited. Systematic basis sets and wave functions. *J. Chem. Phys.* **1992**, *96*, 6796-6806.
17. Sipachev, V. A. Calculation of Shrinkage Corrections in Harmonic Approximation. *THEOCHEM* **1985**, *22*, 143-151.

18. Sipachev, V. A. Local Centrifugal Distortions Caused by Internal Motions of Molecules. *J. Mol. Struct.* **2001**, *567-568*, 67-72.
19. Wann, D. A., Less, R. J., Rataboul, F., McCaffrey, P. D., Reilly, A. M., Robertson, H. E., Lickiss, P. D., Rankin, D. W. H. Accurate gas-phase experimental structures of octasilsesquioxanes ($Si_8O_{12}X_8$; X = H, Me). *Organometallics* **2008**, *27*, 4183-4187.
20. Marenich, A. V.; Cramer, C. J.; Truhlar, D. G. Universal solvation model based on solute electron density and on a continuum model of the solvent defined by the bulk dielectric constant and atomic surface tensions. *J. Phys. Chem. B.* **2009**, *113*, 6378-6396.
21. Neese, F. The ORCA program system. *WIREs Comput. Mol. Sci.* **2012**, *2*, 73-78.
22. Becke, A. D. Density-functional exchange-energy approximation with correct asymptotic behavior. *Phys. Rev. A* **1988**, *38*, 3098-3100.
23. Lee, C.; Yang, W.; Parr, R. G. Development of the Colle-Salvetti correlation-energy formula into a functional of the electron density. *Phys. Rev. B* **1988**, *37*, 785-789.
24. Stephens, P. J.; Devlin, F. J.; Chabalowski, C. F.; Frisch, M. J. Ab initio calculation of vibrational absorption and circular dichroism spectra using density functional force fields. *J. Phys. Chem.* **1994**, *98*, 11623-11627.
25. Becke, A. D. Density-functional thermochemistry. III. The role of exact exchange. *J. Chem. Phys.* **1993**, *98*, 5648-5652.
26. Weigend, F.; Ahlrichs, R. Balanced basis sets of split valence, triple zeta valence and quadruple zeta valence quality for H to Rn: Design and assessment of accuracy. *Phys. Chem. Chem. Phys.* **2005**, *7*, 3297-3305.
27. Grimme, S.; Antony, J.; Ehrlich, S.; Krieg, H. A consistent and accurate *ab initio* parametrization of density functional dispersion correction (DFT-D) for the 94 elements H-Pu. *J. Chem. Phys.* **2010**, *132*, 154104-154119.
28. Grimme, S.; Ehrlich, S.; Goerigk, L. Effect of the damping function in dispersion corrected density functional theory. *J. Comput. Chem.* **2011**, *32*, 1456-1465.
29. Huntley, C. M., Laurenson, G. S., Rankin, D. W. H. Gas-phase molecular structure of bis(difluorophosphino)amine, determined by electron diffraction. *J. Chem. Soc., Dalton Trans.* **1980**, *6*, 954-957.
30. Fleischer, H., Wann, D. A., Hinchley, S. L., Borisenko, K. B., Lewis, J. R., Mawhorter, R. J., Robertson, H. E., Rankin, D. W. H. Molecular structures of

$Se(SCH_3)_2$ and $Te(SCH_3)_2$ using gas-phase electron diffraction and *ab initio* and DFT geometry optimisations. *Dalton Trans.*, **2005**, *19*, 3221-3228.

31. Hinchley, S. L.; Robertson, H. E.; Borisenko, K. B.; Turner, A. R.; Johnston, B. F.; Rankin, D. W. H.; Ahmadian, M.; Jones, J. N.; Cowley, A. H. The molecular structure of tetra-*tert*-butyldiphosphine: an extremely distorted, sterically crowded molecule. *Dalton Trans.* **2004**, 2469-2476.
32. Ross, A. W.; Fink, M.; Hilderbrandt, R. In *International Tables for Crystallography*; Wilson, A. J. C., Ed.; Kluwer Academic Publishers: Dordrecht, Netherlands, 1992; Vol. C, p 245.
33. Sheldrick, G. M. A short history of SHELX. *Acta Cryst. A* **2008**, *64*, 112-122.
34. Sheldrick, G. M. *SADABS*, University of Göttingen, Germany, **1996**.
35. Zink, R.; Hassler, K.; Roth, A.; Eujen, R. The rotational isomerism of $CF_3Me_2SiSiMe_2CF_3$: Do three conformers exist in the liquid state? In *Organosilicon Chemistry IV – From Molecules to Materials*, Auner, N.; Weis, J. Eds.; Wiley-VCH: Weinheim, **2000**.
36. Beagley, B.; Monaghan, J. J.; Hewitt, T. G. Electron-diffraction studies of tetramethylsilane and hexamethyldisilane, and discussion of the lengths of Si-C bonds. *J. Mol. Struct.* **1971**, *8*, 401-411.
37. Beagley, B.; Conrad, A. R.; Freeman, J. M.; Monaghan, J. J.; Norton, B. G.; Holywell, G. C. Electron diffraction studies of the hydrides Si_2H_6 and P_2H_4. *J. Mol. Struct.* **1972**, *11*, 371-380.

■ GRAPHICAL ABSTRACT

The molecular structure of 1,2-bis(trifluoromethyl)-1,1,2,2-tetramethyldisilane has been elucidated in the solid state, solution phase, and gas phase; the solid-state and gas-phase experiments indicate that only one conformer is present, whilst in the solution phase three conformers are stabilized by the solvent.

Number of conformers

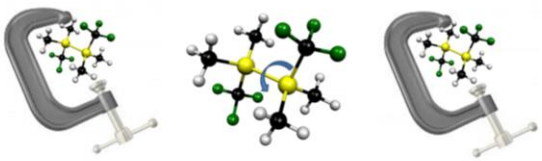

Solid	Solution	Gas
1	3	1